Tellus (1990), *42A*, 51–64

Time-mean precipitation and vertical motion patterns over the United States

By H. M. VAN DEN DOOL, *Cooperative Institute for Climate Studies, University of Maryland, College Park, MD 20742, USA*

(Manuscript received 1 November 1988; in final form 10 May 1989)

ABSTRACT

A post-initialized set of global atmospheric gridded data, generated at NMC, is used to calculate monthly mean vertical motion at 500 mb ($\overline{\omega}$) for all months in 1984–1986. Various methods are used to calculate $\overline{\omega}$ such as those based on the continuity (the best and easiest) and vorticity equations. The $\overline{\omega}$ fields are correlated with colocated monthly precipitation (P) collected in raingauges and averaged over Climate Divisions in the United States. The correlation between $\overline{\omega}$ and P for the United States as a whole is negative (to be hoped), the coefficient ranging from about -0.6 in winter to small negative values in summer. Statistical significance is reached in 10 out of 12 months. The vorticity equation is used to decompose $\overline{\omega}$ into contributions from mean flow- and transient eddy vorticity fluxes, respectively. Using mean flow fluxes alone leads to highly overestimated $\overline{\omega}$ (compared to continuity), but the spatial pattern over the United States is essentially correct. The transient eddy fluxes are smaller by a factor of two and nearly opposite (correlation ≈ -0.8) to the mean flow fluxes, and seem to "force" vertical motions that are roughly out of phase with the precipitation field (correlation ≈ 0.0). Using mean flow fluxes only and accepting geostrophic constraints, the results deteriorate, although P and $\overline{\omega}$ remain negatively correlated at modest levels for all months. The above results are true for 3-year monthly means ("climatology") as well as for departures from climatology (anomalies). The impact of the initialization on $\overline{\omega}$ is small, and the impact on the P, $\overline{\omega}$ correlation almost negligible. Statistics for the 3-year period, and some examples in map-form are presented. Furthermore the geographical distribution of the P, $\overline{\omega}$ correlation is discussed using data for 1981–86.

1. Introduction

It is well known that precipitation (P) in mid-latitudes is associated with large-scale transients, particularly in winter. One would therefore expect that transients play an important role in the maintenance of the time-mean precipitation field. Remarkably, however, a good deal of information about monthly precipitation patterns has been inferred from monthly mean 700 mb height alone (Klein and Bloom, 1987), without explicit reference to transient variability on shorter time-scales.

Studying maintenance or budget equations was without any doubt the cornerstone of General Circulation Studies in the 1940s and 50s. Usually, the budget equation was applied to such fields as time mean (and/or zonal mean) momentum; the maintenance of the mid-latitude westerlies is a famous example (Palmén and Newton, 1969, Ch. 1). The role of transient eddies has been greatly clarified through these observational studies.

We don't know of any equation $\mathrm{d}P/\mathrm{d}t$ so a study of the budget of P is not as straightforward as that for zonal wind. Because we believe P to be intimately related to vertical motion (p velocity, ω, that is), we will instead address the "maintenance" of time-mean ω, i.e., $\overline{\omega}$. Because of the hydrostatic assumption there is no equation $\mathrm{d}\omega/\mathrm{d}t$ either, but at least ω is a non-discontinuous quantity related to the other fields (mass, horizontal wind) through the governing equations. We will study here $\overline{\omega}$ through the continuity equation, and through the vorticity equation. In the continuity equation, $\overline{\omega}$ is linearly related to the horizontal wind and no explicit impact of transient eddies can be seen. On the other hand, in the vorticity equation, $\bar{\omega}$ is derived from non-linear vorticity advection, allowing us to separately study the role of transient eddies and mean flow in balancing the stretching term.

The purpose of this paper is as follows. First to establish that with current large-scale data sets monthly mean vertical motion is demonstrably related to monthly mean precipitation, at least over the United States. Second to show that, given a modern data set consisting of model initial states, the correct $\bar{\omega}$ can be retrieved rather easily by using the continuity equation, and with some more trouble and less accuracy also from the vorticity equation. Thirdly, to show that in all 36 months in the 1984–86 period studied here, the vorticity flux by transient eddies is roughly the opposite, and half the magnitude, of the vorticity flux by the mean flow. Therefore, if one uses only mean flow fluxes, the resulting vertical motion field would be overestimated in magnitude but essentially correct in pattern. And lastly, that because geostrophic mean flow vorticity fluxes correlate highly (0.8 or higher) with vorticity fluxes based on observed winds, the vertical motion derived from geostrophic winds is only slightly less reliable (in its correlation with precipitation, our ground truth) than that derived from observed winds.

In the description that follows, most emphasis is on interannual variability of monthly mean P and ω (the latter at 500 mb!; other levels give comparable but very slightly worse results) over the United States, relative to a 1984–86 monthly mean. The vorticity budget of long-term mean flow has been described by Holopainen and Oort (1981), and will be discussed here only for comparison. The relation between P and ω over the United States during 1981–83 was discussed in Van den Dool (1987). Combining the 1981–83 and 84–86 data the geographical distribution of the (P, ω) correlation will be discussed as well.

2. Data and analysis

We use data for the period 1984–86, from the following two datasets.

(i) Spatially averaged monthly precipitation (P) for 344 Climate Divisions (CD) in the United States.

(ii) Monthly accumulated data on a global $2.5° \times 2.5°$ latitude-longitude grid, the so-called Climate Diagnostics Data Base (CDDB). The CDDB contains averages, variances and co-variances based on twice daily post-initialized data produced routinely for global Numerical Weather Prediction (NWP) at the National Meteorological Center (NMC) in Washington, DC and archived by NMC's Climate Analysis Center (CAC). Fields that we will use here are vertical motion at 500 mb ($\bar{\omega}$), and $\bar{u}$, $\bar{v}$, $\bar{Z}$, $\overline{u\zeta}$, $\overline{v\zeta}$, at all levels above and including 500 mb. (u, v are zonal and meridional wind, Z is height of pressure surface, and ζ is relative vorticity; the bar is a monthly mean). In 1984, 85 and 86 the percentage of missing data was 6.5%, 3.0% and 1.3% respectively. Missing data means that all fields at all levels are missing for that time.

In a given year j and month m we can express the similarity of anomalies in the fields of vertical motion ($\omega(m, j)$) and precipitation ($P(m, j)$) by employing a pattern correlation coefficient

$$\mathrm{PC}(m,j) = \left\{\frac{1}{344}\sum_{c=1}^{344} \hat{\omega}(m,j,c)\,\hat{P}(m,j,c) - [\hat{\omega}(m,j,c)][\hat{P}(m,j,c)]\right\} \times [\mathrm{sd}_{\omega}(m,j)\,\mathrm{sd}_{\mathrm{pp}}(m,j)]^{-1}, \quad (1)$$

where c is an index for the climate divisions, brackets represent a continental wide average, the caret represents the departure from a local, 3-year mean for month m, and the standard deviation (sd) in the denominator of (1) is given by

$$\mathrm{sd}_{\omega}(m,j) = \left\{\frac{1}{344}\sum_{c=1}^{344} [\hat{\omega}(m,j,c) - [\hat{\omega}(m,j,c)]]^2\right\}^{1/2},$$

and similarly for sd_{p}. In (1), all CDs are given equal weight, even though we realize that their sizes are different (see Janowiak et al., 1986 for a map of CDs). When all terms in (1) are summed through over the 3 years, a simpler pattern correlation emerges:

$$\mathrm{PC}(m) = \frac{\sum_{c=1}^{344}\sum_{j=1}^{3} \hat{\omega}(m,j,c)\,\hat{P}(m,j,c)}{\left\{\sum_{c=1}^{344}\sum_{j=1}^{3} \hat{\omega}(m,j,c)^2 \sum_{c=1}^{344}\sum_{j=1}^{3} (\hat{P}(m,j,c))^2\right\}^{1/2}}, \quad (1a)$$

which is only a function of the month m. In eq. (1a), all continental averages have vanished. Hereafter we will use mostly (1a). In order to apply (1) or (1a), the ω values, calculated originally on the grid, were interpolated so as to colocate with the P data assigned to the centroids of the 344 CDs.

Seven methods are used to calculate the mean vertical motion. It is important to emphasize here that we try to calculate *monthly mean* vertical motion. This long enough time average makes the time derivative in most equations small if not negligible (ignoring in particular the models' "climate drift" which enters through the guess fields), see Opsteegh and Van den Dool (1979).

Method c (continuity)

This is the time mean (average over 56, 58, 60 or 62 cases (or less when data is missing)) of twice daily vertical motion derived from NMC initialized analyses and archived in real time at CAC. Application of the continuity equation in σ coordinates to monthly mean u, v would be the easiest way to calculate this $\bar{\omega}$, hence the name—Method c. (But since the data were archived already, we did not have to do the calculation). Calculating $\bar{\omega}$ according to Method c yields the best answer we can possibly expect.

Method cp (continuity p coordinates)

The NMC-CAC post-processor saves data inter/extrapolated to 9 p surfaces (as of 1988, 18 sigma levels are available in principle). So our closest copy of Method c is to apply the continuity equation to (u, v) at p surfaces, that is

$$\frac{\partial\bar{\omega}}{\partial p} = -\left(\frac{\partial\bar{u}}{\partial x} + \frac{\partial\bar{v}}{\partial y} - \frac{\bar{v}\tan\phi}{a}\right) = D_{\text{cp}}, \qquad (2)$$

where a is the radius of the earth, D is the horizontal divergence evaluated in spherical coordinates and the bar represents a monthly mean. Knowing D_{cp} at 50, 100, 200, 250, 300, and 500 mb, assuming $\bar{\omega}$ (25 mb) = 0 and integrating downward to 500 mb yields $\bar{\omega}$ at 500 mb. As it turns out, Methods c and cp yield vertical motions at 500 mb that are usually very close, thereby indicating that the σ to p coordinate conversion, in this context, is only a minor problem. Also, it validates $\bar{\omega}$ (25 mb) = 0 as an appropriate upper boundary condition to be used in this and all subsequent methods.

Method a (vorticity *a*dvection)

In this case $\bar{\omega}$ is derived from

$$\frac{\partial\bar{\omega}}{\partial p} = \frac{1}{(\bar{\zeta}+f)}\left(\bar{u}\frac{\partial\bar{\zeta}}{\partial x} + \bar{v}\frac{\partial\bar{\zeta}}{\partial y} + \bar{v}\frac{\partial f}{\partial y} + \gamma\bar{\zeta}\right) = F_{\text{a}}, \quad (3)$$

where vorticity is given by:

$$\bar{\zeta} = \frac{\partial\bar{v}}{\partial x} - \frac{\partial\bar{u}}{\partial y} + \bar{u}\frac{\tan\phi}{a},$$

and f is the Coriolis parameter.

In (3), we assume that the divergence term balances the horizontal advection of absolute vorticity. Note that u and v are observed winds containing irrotational components. The added linear damping ($\gamma = 10^{-6}\ \text{s}^{-1}$) was originally thought to be an improvement but no noticeable change in the correlation with simultaneous precipitation occurred. Knowing F_{a} at 50, 100, 200, 250, 300 and 500 mb we can then integrate (3) downward, assuming again $\bar{\omega}$ (25 mb) = 0. Method a has recently been applied by Savijärvi (1977), Lau (1979) and White (1983) but has never been compared systematically to other estimates of vertical motion or precipitation. (The idea to extract ω from the vorticity equation is much older (Eliassen and Hubert, 1953).)

Method f (vorticity *f*lux)

Here $\bar{\omega}$ is calculated from

$$\frac{\partial\bar{\omega}}{\partial p} = \frac{1}{f}\left(\frac{\partial}{\partial x}\overline{u\zeta} + \frac{\partial}{\partial y}\overline{v\zeta} + \bar{v}\frac{\partial f}{\partial y} + \gamma\bar{\zeta}\right) = F_{\text{f}}, \qquad (4)$$

a method almost identical to Method a. Method f is less desirable because $\bar{\zeta}\,\partial\bar{\omega}/\partial p$ is absorbed into the flux. That is, in (4) an $\bar{\omega}$ is implicitly used in the fluxes that may be slightly different from $\bar{\omega}$ that we want to solve for. However, the intermediate Method f is necessary for later comparison to Method fe because of the way the General Circulation Statistics are stored at CAC, i.e.,

$$\left(\bar{u}, \bar{\zeta}, \overline{u\zeta}, \text{rather than } \bar{u}, \bar{\zeta}, \bar{u}\frac{\partial\bar{\zeta}}{\partial x}, \overline{u'\frac{\partial\zeta'}{\partial x}}\right).$$

Knowing F_{f} at 50, 100, 200, 250, 300 and 500 mb, we can integrate (4) downward assuming $\bar{\omega}$ (25 mb) = 0. As we will see below Methods a and f are virtually identical in practice.

Method fe (vorticity *f*lux plus *e*ddies)

As Method *f* but now including the transient eddies:

$$\frac{\partial \bar{\omega}}{\partial p} = \frac{1}{f}\left(\frac{\partial}{\partial x}\overline{u\zeta} + \frac{\partial}{\partial y}\overline{v\zeta} + \bar{v}\frac{\partial f}{\partial y} + \gamma\bar{\zeta}\right) = F_{\mathrm{fe}}, \quad (5)$$

integrated, as before, from 25 mb down to 500 mb. Method *fe* is the most complete version of the vorticity approach reported here. (Unfortunately the $\overline{u\zeta}$ and $\overline{v\zeta}$ quantities were not archived at 50 and 100 mb and replaced, for our purpose, by $\bar{u}\bar{\zeta}$ and $\bar{v}\bar{\zeta}$.)

With a dynamically consistent data set, eq. (5) should yield approximately the same $\bar{\omega}$ as Method *c*. And it does, but not until heavy smoothing is applied. The smoothing is necessary because the data is archived at vertical and horizontal grids that are inconsistent with the representation of the model that generated the data before it was postprocessed. Nevertheless, even with perfect archiving, some differences would remain because of approximations in (5) and because the dynamical consistency is not perfect. The latter is probably a more serious problem in the tropics (Sardeshmukh and Hoskins, 1987).

Method e (vorticity flux by transient *e*ddies alone)

The difference between Methods *f* and *fe*, i.e., ((5)–(4))

$$\frac{\partial \bar{\omega}}{\partial p} = \frac{1}{f}\left(\frac{\partial}{\partial x}\overline{u'\zeta'} + \frac{\partial}{\partial y}\overline{v'\zeta'}\right) \quad (6)$$

is integrated, as before, from 25 mb down to 500 mb. Here, the prime denotes departure from monthly mean. Comparison of Methods *f* and *e* will highlight the role of transient eddies (relative to the time-mean flow advection) in balancing the divergence term. Methods *fe* and *e* can be evaluated over 1984–86 only, due to an, until then, undiscovered error in the archiving process at CAC of the eddy vorticity terms through 1982. As discussed under Method *f*, contributions due to transient eddies can not be evaluated at level 50 and 100 mb due to archiving problems.

Method g (*g*eostropic vorticity advection)

As Method *a* except that winds and vorticity are calculated geostrophically from the height fields, i.e.,

$$\frac{\partial \bar{\omega}}{\partial p} = \frac{1}{f_0}\left(\bar{u}_{\mathrm{g}}\frac{\partial \bar{\zeta}_{\mathrm{g}}}{\partial x} + \bar{v}_{\mathrm{g}}\frac{\partial \bar{\zeta}_{\mathrm{g}}}{\partial y} + \bar{v}_{\mathrm{g}}\beta + \gamma\bar{\zeta}_{\mathrm{g}}\right) = F_{\mathrm{g}}, \quad (7)$$

where a β-plane has been assumed relative to 40°N. Eq. (7) is interesting mostly for historical reasons (perhaps one could retroactively apply (7) to height fields back into the 1940s and 50s), or to assess whether the vorticity advection by the irrotational winds in (3) has a noticeable impact on the resulting estimate of the forcing F_{a} and ultimately $\bar{\omega}$. The latter problem is a key issue in Sardeshmukh and Hoskins (1987) who sought to calculate the divergence from the vorticity equation while specifying the rotational wind.

The various approaches outlined here all have slightly different noise problems. So some filtering is needed especially on the vorticity approach. Table 1 specifies the pre- and post-processing as well as the numerical schemes used to arrive at the estimate for $\bar{\omega}$ at 500 mb, for all methods, *a*, *f*, *fe*, *e*, *g*, *c* and *cp*.

The familiar ω equation (Holton, 1979, p. 137), or the *Q*-vector approach (Hoskins et al., 1978) are of no particular use here because they are derived by eliminating the time derivative between the geostrophic vorticity and thermodynamic equation. Since the time derivatives are very small for monthly means, one does better to use either the vorticity or the thermodynamic equation directly. As was pointed out by Zwack and Okossi (1986), the vorticity equation (our Method *g*) is preferable as it does not depend on knowing the heating. Mullen (1986) did apply Holton's ω equation to a composite blocking case and found good results. The geostrophic vorticity equation alone should have done equally well or better and is much easier to solve.

The Methods *a*, *f*, *fe*, *e*, and *g* should be judged in view of the complete vorticity equation:

$$0 = \frac{\partial \bar{\zeta}}{\partial t} = \left.\begin{array}{l} -\dfrac{\partial}{\partial x}\overline{u\zeta} + \dfrac{\partial}{\partial y}\overline{v\zeta} - \bar{v}\dfrac{\partial f}{\partial y} - \gamma\bar{\zeta} \\ -\dfrac{\partial}{\partial x}\overline{u'\zeta'} - \dfrac{\partial}{\partial y}\overline{v'\zeta'} \end{array}\right\}\mathrm{I}$$

$$\left. + f\frac{\partial \bar{\omega}}{\partial p} \right\}\mathrm{II}$$

Table 1. *Overview of the pre- and postprocessing, and numerical schemes applied to calculate vertical motion according to the methods a, f through cp*

Stage \ Method	*a*	*f*	*fe*	*e*	*g*	*c*	*cp*
preprocessor fields	T27HS u, v	T27HS, and 1-2-1 u, v	(1-2-1) (u, v)	none	T27HS Z	(--)	none
numerical scheme	4th order	2nd order	(2nd order)	none	4th order	(--)	4th order
postprocessor fields	none	none	T27HS ω	$e = fe - f$ ω	none	1-2-1 ω	1-2-1 ω

Z, u, v, ω are height, zonal, meridional and vertical wind fields. T27HS is a smooth spectral truncation at total wavenumber 27 (see Hoskins and Sardeshmukh (1987)) and the 1-2-1 filters are applied simultaneously in both horizontal directions (a 5 point filter). The operations in parentheses are applied in real time during the archiving of the data and cannot be changed retroactively. The dashes in parentheses under Method *c* stand for all operations associated with analysis and initialization.

$$\left.\begin{aligned} &-\bar{\omega}\frac{\partial\bar{\zeta}}{\partial p}+\left(\frac{\partial\bar{u}}{\partial p}\frac{\partial\bar{\omega}}{\partial y}-\frac{\partial\bar{v}}{\partial p}\frac{\partial\bar{\omega}}{\partial x}\right)\\ &-\overline{\omega'\frac{\partial\zeta'}{\partial p}}+\left(\overline{\frac{\partial u'}{\partial p}\frac{\partial\omega'}{\partial y}}-\overline{\frac{\partial v'}{\partial p}\frac{\partial\omega'}{\partial x}}\right).\end{aligned}\right\}\text{III}$$

What we do in Methods *a*, *f*, *fe*, *e* is to calculate terms not involving direct knowledge of vertical motion in group I (with varying degrees of completeness) and to equate them to term II. This approach would be a failure if the terms under III are non-negligible. We, in fact, were able to include $\bar{\omega}\partial\bar{\zeta}/\partial p$ directly into the *fe* method. As it turns out, the mean flow vertical vorticity advection is entirely negligible in the mid-latitudes. It is possible to include the twisting term although it would require iteration involving neighboring gridpoints, but it would seem that the twisting term has to be very small too. Only the eddy correlations involving vertical motion remain; they are essentially unknown. Some additional observational support for equating term II to group I has recently come from high resolution wind profiler measurements (Zamora et al., 1987).

3. Results

In the first line of Table 2 we present PC(c, P), that is the correlation for monthly anomalies over the United States, 1984–86, between vertical motion at 500 mb ($\bar{\omega}$, according to Method *c*) and precipitation collected in raingauges (P). $\bar{P}$ and $\bar{\omega}$ are measured/calculated in truly independent ways, as rainfall data are not (yet) used in initializing the NWP models. The correlation is negative (to be hoped) in all months, and the values range from about -0.65 in winter to modest negative values in summer. In 10 out of 12 months, the correlation is significant according to a one-sided t-test (see Appendix). This is an important result. The same level of correlation was found for 1981–83 (Van den Dool, 1987), so there is no drastic improvement in the correlation in spite of the many model improvements since 1983. Indeed, the nature of the P observations may limit further increase in correlation.

In the second line of Table 2, we present PC(c, cp) the correlation between our presumably best estimate of vertical motion (c, i.e., Method c) and the one obtained from applying the continuity equation in p coordinates. There is no doubt that the *cp* method does a nearly perfect job in winter in retrieving ω from u, v even though we use model-inconsistent vertical and horizontal coordinate systems and too few levels in the vertical. The correlations are not perfect, i.e., only 0.75, in summer. This level of agreement between c and cp in summer was reached only after we started using 4th-order accurate horizontal differencing to calculate divergence (see Table 1).

In view of the high PC(c, cp) it is not surprising that *cp* correlates well with precipitation, see PC(cp, P) in the third line of Table 2. In fact *cp*

Table 2. *The pattern correlation (%) between monthly precipitation (P) and vertical motion anomalies over the United States, 1984–86, as a function of month*

Month	J	F	M	A	M	J	J	A	S	O	N	D
PC(c, P)	−38*	−47*	−44*	−54*	−41*	−8	−39*	−17	−53*	−39*	−65*	−61*
PC(c, cp)	94	87	87	92	92	78	72	74	76	94	95	90
PC(cp, P)	−44*	−57*	−32*	−47*	−45*	−18	−29*	−25*	−49*	−38*	−61*	−56*

The methods of calculating vertical motion (c, cp) are described in Section 2. The PC is defined by (1a). The asterisk denotes statistical significance according to a one-sided t-test (see appendix).

Table 3. *As Table 2 but for method fe instead of cp*

Month	J	F	M	A	M	J	J	A	S	O	N	D
PC(c, P)	−38*	−47*	−44*	−54*	−41*	−8	−39*	−17	−53*	−39*	−65*	−61*
PC(c, fe)	71	52	64	41	67	51	32	56	64	73	75	70
PC(fe, P)	−27*	−24	−25*	−29*	−47*	−17	−22	−34*	−32*	−23	−58*	−53*

scores 11 (out of 12) significant correlations and PC(cp, P) is not visibly worse than PC(c, P).

Having established that interannual variability in monthly mean, ω and P are reasonably correlated, we now move on to study ω in the context of the vorticity equation. This entailed a *major* struggle with horizontal filters, differencing schemes and accepting problems with the way data were treated at the time of archiving. For obvious reasons, the vorticity method is far more sensitive to "noise" (or perhaps real physical small scales) than the continuity method. Hence heavier filtering was applied, see Table 1. We decided a priori that all months would be treated in the same way. So a smooth spectral truncation at total wavenumber 27 (the T27HS filter see Table 1; Hoskins and Sardeshmukh, 1987) is applied in all 36 months. The results in winter (in terms of correlation with P over the United States) would probably improve from more severe filtering while the reverse is true in summer. The results are presented in Table 3, which is as Table 2 but with fe replacing cp. There is no doubt that fe is at best a reasonable substitute for c (or cp), the PC(c, fe) values ranging from acceptable in winter (0.7) down to very low in summer ($\sim$0.3). Nevertheless, PC(fe, P) is negative in all months and statistically significantly so in 8 (out of 12) months. Thus, an as-complete-as-possible version of the vorticity equation applied with great care for the numerics does yield a proxy for vertical motion that correlates with precipitation. We don't think that much further improvement can be made here because the data were not stored in a model-consistent manner. With much stronger filtering (say T15HS), the PC(c, fe) increases, but PC(fe, P) simultaneously goes down to zero. This happens because the horizontal scales at which P and ω correlate well are rather small, especially in summer. Unfortunately some "noise" due to sigma-to-p-coordinate transforms is present at the same scales.

The results so far are visually summarized in Fig. 1, where PC(c, P) PC(cp, P) and PC(fe, P) are plotted. We see generally poorer correlations in summer when convection is predominant. The Methods c and cp yield just about equal results, while fe performs worse in most winter months.

Given that the correlation PC(fe, P) is negative and significantly so in 8 out of 12 months, see Table 3, the question can be asked as to what would happen if we ignore transient eddy effects. In Table 4 (upper part) and Fig. 2, we present PC(f, P), PC(e, P) and PC(fe, P). From this comparison, it is obvious that the inclusion of the transient eddies in balancing fD is indeed quite

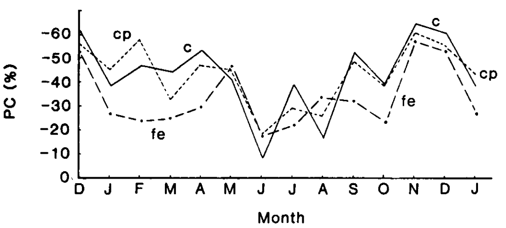

Fig. 1. The pattern correlation (PC in %) between precipitation anomalies and vertical motion ($\overline{\omega}$) anomalies over the United States 1984–1986, as a function of the time of year. The PC is calculated according to (1a). Precipitation (P) is correlated with $\overline{\omega}$ calculated according to Method c (full line), Method cp (dashed line), and Method fe (dashed-dot line).

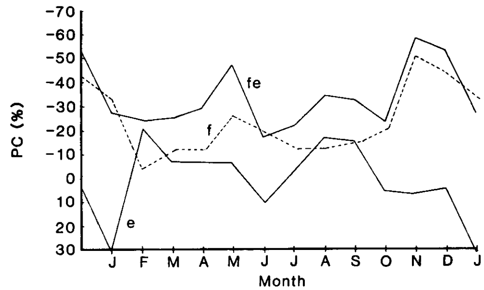

Fig. 2. As Fig. 1 but now P correlated with $\overline{\omega}$ according to Method fe (full), Method f (dashed), Method e (full).

Table 4. *The pattern correlation (%) between monthly precipitation and vertical motion anomalies at 500 mb over the United States, 1984–86*

Month	J	F	M	A	M	J	J	A	S	O	N	D
PC(f, P)	−33*	−4	−12	−11	−26	−18	−12	−13	−14	−20	−51*	−43*
PC(e, P)	31	−21	−7	−7	−6	11	−2	−17	−15	6	7	4
PC(fe, P)	−27*	−24	−25*	−29*	−47*	−17	−22	−34*	−32*	−23	−58*	−53*
PC(f, e)	−81	−55	−76	−84	−75	−80	−81	−67	−59	−71	−60	−64
RMS(f)	4.3	2.1	3.3	2.7	2.3	2.5	1.6	1.4	1.6	2.3	3.5	3.2
RMS(e)	2.0	1.6	2.2	2.2	1.8	1.7	1.3	1.2	1.4	1.4	1.9	1.7
RMS(fe)	2.9	1.8	2.1	1.5	1.5	1.5	0.9	1.0	1.4	1.6	2.8	2.5
RMS(c)	1.9	1.7	1.5	1.3	1.3	1.2	0.8	1.0	1.4	1.7	2.6	1.7

The methods of calculating ω (f, e, fe) are all based on the vorticity equation. In the lower portion RMS values are tabulated, i.e., root-mean-square of vertical motion anomalies, summed over all locations (344) and years (3) according to methods f, e, fe and c; the unit is 10^{-2} N m^{-2} s^{-1}. The RMS measures interannual variability.

important. The (f, P) correlation is significant only in 3 winter months, while PC(fe, P) is significant in 8 months. Remarkably, the PC(e, P) on its own is about zero the whole year round. Apparently the upward motion "caused" by explicit transient eddy vorticity transport is not (linearly) related to the rainfall anomaly pattern. This remarkable and counter-intuitive fact is better understood after studying the lower portion of Table 4. Since PC(f, e) is highly negative, it follows that the vorticity fluxes by the mean flow and transient eddies tend to be opposite (at least over the USA), so much so that the magnitude of fe (as measured by spatial RMS) is considerably less than that of f alone. Apparently, the mean flow advection leads to a seriously overestimated $\overline{\omega}$, and the transient eddies correct for that. Note that the RMS magnitudes of fe, e and c are all quite close. This implies that transient eddies account for the entire interannual variability of $\overline{\omega}$ as far as amplitude is concerned. But the patterns in ω "forced" by eddies alone are different from those observed.

As an example, we have chosen December 1984. Figs. 3a through 3e display maps of anomalies (relative to the 3-year monthly mean) in the following fields: precipitation, c (i.e., $\overline{\omega}$ acc. to Method c), fe, f and e. There are large excesses and deficits in P over the Eastern half and

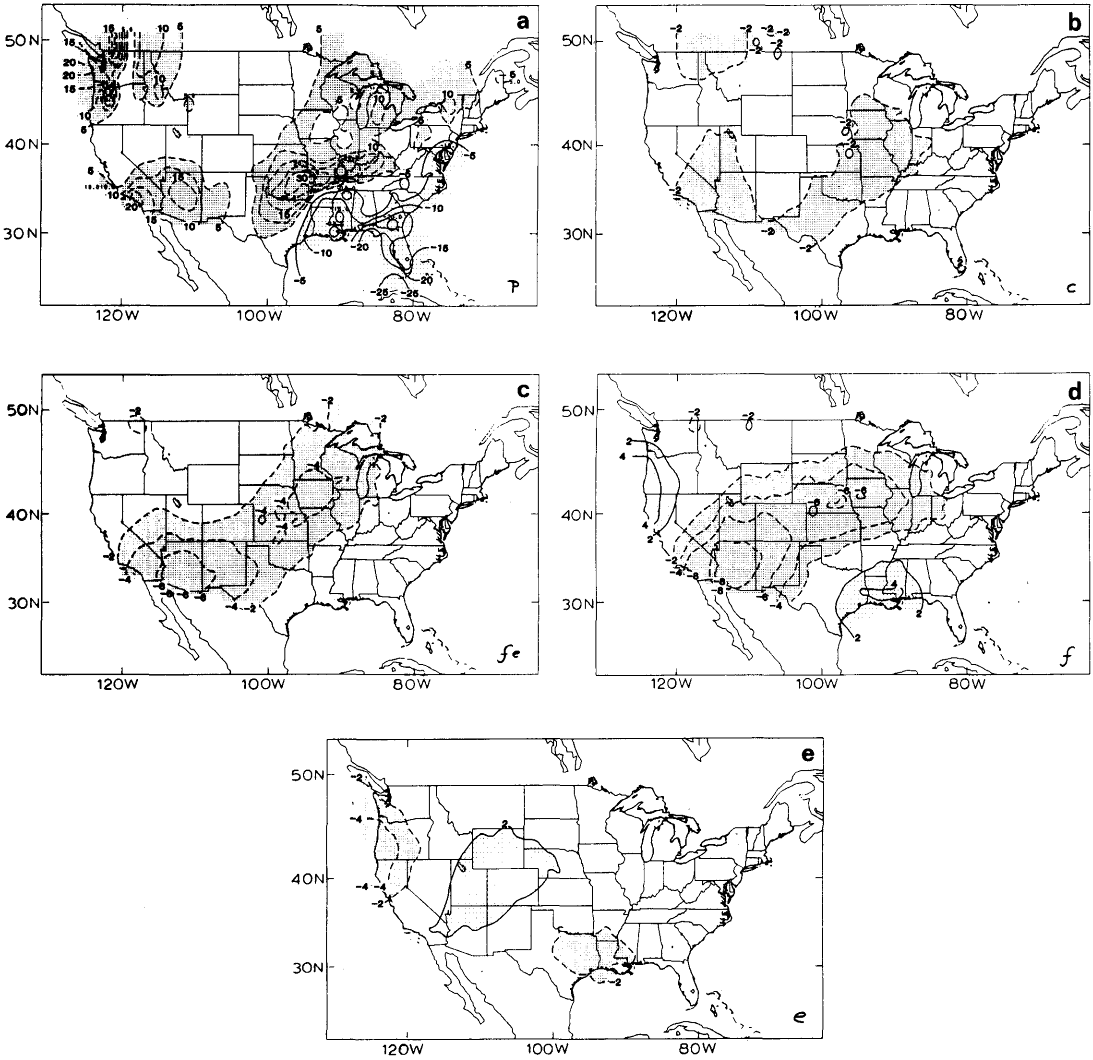

Fig. 3. Anomalies, i.e., departure from 3-year monthly mean, in December 1984 for precipitation (3a), $\bar{\omega}$ acc (ording) to Method *c* (3b), $\bar{\omega}$ acc to Methods *fe*, *f* and *e* (3c, 3d and 3e). For $\bar{\omega}$ the unit is 10^{-2} N m^{-2} s^{-1}, for *P* 10^{-1} mm day^{-1}. Rising motion <-2 units is heavily dotted, descending motion $>+2$ units is lightly dotted. Rainfall $>+5$ units is heavily dotted, rainfall <-5 units is lightly dotted. Negative (positive) contours of $\bar{\omega}$ are dashed (full), contour interval 2 units, zero contour omitted. Negative (positive) contours of *P* are full (dashed), contour interval 5 units, zero contour omitted.

extreme western part of the United States. This *P* anomaly field has a high degree of similarity with the *c* anomalies (Fig. 3b), although the linear correlation, using eq. (1), is just -0.63 (similar to Table 2 values). But there is no doubt that anomalous upward (downward) motion goes along with too much (little) precipitation. Going from Method *c* to *fe* (i.e., Fig. 3b to 3c) decreases the spatial match slightly. In particular, the vorticity advection implies too strong upward vertical motion too far west. PC(fe, P) is -0.57 down from -0.63 (PC(c, P)). When utilizing time-mean fields only (Method *f*, Fig. 3d), the magnitude becomes much too large and also the pattern shifts in the wrong (westward) direction. Hence PC(f, P) is only -0.43. The compensating part of $\bar{\omega}$, due to eddies alone is shown in Fig. 3e. Fig. 3e is correlated highly negatively with Fig. 3d (-0.78). The e field is in quadrature with P; hence PC(e, P) $= 0.10$.

Before 1980, an analysis as presented here would have been impossible because of a lack of properly assimilated/balanced data on a global scale. Holopainen and Oort (1981) refrain from calculating ω in their study based on radiosonde wind data (1968–73) and Lau (1979) and White (1983) use 6-h forecasts as proxies of balanced ω observations. But at least a quasi-geostrophic estimate would have been available from height analyses, essentially our Method g. In Table 5, we compare Methods a and g, both in their correlation with precipitation and in the magnitude of calculated ω's. In 10 out of 12 months, the a Method correlates better to precipitation than g, although the difference is not very large. So QG theory in mid-latitudes is a reasonable approximation. (This conclusion is overstated to the extent that the constraints used in the Optimum Interpolation analysis at NMC force winds and heights more into geostrophic equilibrium than they really are.) It is in only 1 winter month (December) that the advection of vorticity by the ageostrophic wind seems important enough to make a big difference in the retrieved ω. Although the patterns of a and g are very similar (correlation ~ 0.9), the geostrophic method makes for a considerable magnitude error, see the RMS (a) and RMS (g) lines in Table 5. Geostrophic advection is an overestimation because over most of the United States the upper tropospheric flow is cyclonic (i.e., subgeostrophic). The CDDB archive did not allow us to include transient eddies into the geostrophic estimates, but unpublished calculations by D. R. Bolvin (University of Maryland) based on 1963–1977 NMC height fields indicate the same strong compensation between mean flow-geostrophic and transient eddy fluxes. We also note, compare Tables 4 and 5, that the Methods a and f yield nearly identical results.

In this paper, as well as Van den Dool (1987) for 1981–1983, we have presented correlations for the United States as a whole. Combining the data for Method c and P over 6 years, 1981–1986, and defining winter (summer) as November–April (May–October) we have 36 pairs of ($P, \bar{\omega}$) data at each CD. That is just about enough to calculate local temporal correlations which can be contoured to show the geographical distribution. The result is shown in Fig. 4; winter (summer) on top (bottom). Conclusions are that the correlation is negative in both seasons almost everywhere. This is better than expected, especially in summer. Poor correlations are found in very dry climates (much of the Southwest in summer and winter) mainly because negative P anomalies are impossible in many months. The better correlations (< -0.60) in winter are found over the western part of the United States (better than -0.80) and in the upper mid-west (better than -0.70). This map (Fig. 4 top) has a great deal of similarity with Klein and Bloom's (1987) Fig. 7 showing the explained variance of precipitation anomalies obtained by screening the monthly mean 700 mb height maps. This reinforces our impression that to a large extent, screening time-mean heights leads to a vorticity advection type estimate of local $\bar{\omega}$, which, due to the employed regression, is not an overestimate.

Table 5. *The pattern correlation (%) between monthly precipitation and vertical motion (at 500 mb) anomalies over the United States, 1984–86*

Month	J	F	M	A	M	J	J	A	S	O	N	D
PC(a, P)	−33*	−3	−14	−13	−27	−17	−18	−15	−6	−18	−52*	−35*
PC(a, g)	78	85	90	95	91	92	86	90	81	87	92	71
PC(g, P)	−27	0	−16	−5	−25	−10	−16	−3	2	−12	−54*	−18
RMS(a)	4.6	2.4	3.5	2.8	2.5	2.9	2.0	1.6	1.8	2.7	3.8	3.5
RMS(g)	4.6	3.6	4.3	4.4	3.2	3.4	2.3	1.7	2.4	3.7	4.4	4.6

The methods of calculating ω involve vorticity advection (a) and geostrophic vorticity advection (g).The unit of root-mean-square of vertical motion anomalies is 10^{-2} N m^{-2} s^{-1}.

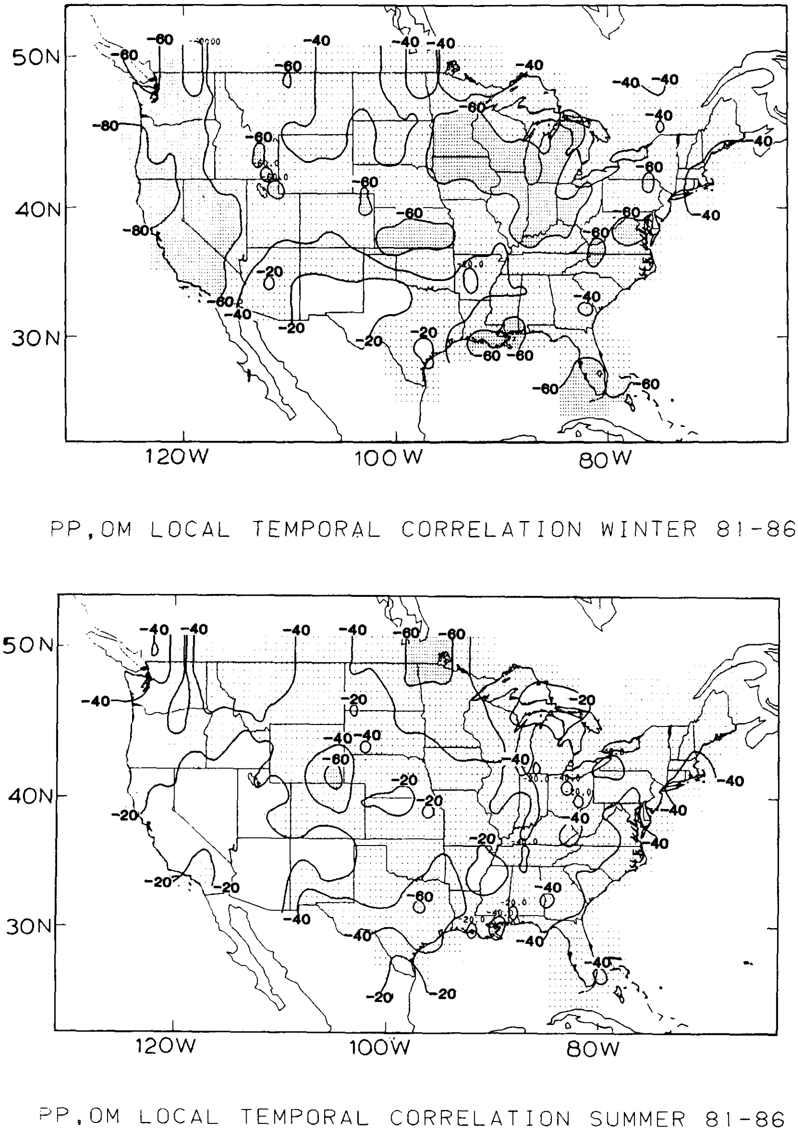

Fig. 4. Geographical distribution of local temporal correlation (%) between anomalies in P and ω (acc to Method *c*). Top: winter (November through April); bottom: summer (May through October). Areas with correlation between -20 and -40% are lightly stippled, beyond -60% heavy stippling is applied. The contour interval is 20%.

4. Conclusions and discussion

A 3-year (1984–86) set of NMC gridded post-initialized data has been used to study the relationship between colocated monthly mean vertical motion at 500 mb ($\bar{\omega}$) and monthly precipitation amount (P) at 344 Climate Divisions in the United States. The conclusions are as follows.

(1) Taking a monthly mean over twice daily vertical motion generated in the initialization step (Method *c*) yields an $\bar{\omega}$ that is negatively correlated with P. Over the United States, the

correlation is moderately good in winter (~ -0.6) and small but negative in summer. The correlation is statistically significant in 10 out of 12 months.

(2) A good proxy for Method c can be obtained by integrating the continuity equation down from $p = 25$ mb, using monthly mean horizontal winds at only 6 pressure levels as input, i.e., Method cp, see Table 2. The match is not perfect because the data are not stored in a model-consistent manner.

(3) Applying the vorticity equation to estimate $\overline{\omega}$ (Methods a, f, fe and e) yields only moderate agreement with Method c. Still, in 8 out of 12 months, the correlation between $\overline{\omega}$ (Method fe) and P is statistically significant (see Table 3, Fig. 2). Because of the higher-order derivatives, the success of Method fe depends very much on filtering the input monthly mean horizontal winds. To a lesser degree, the lack of perfect dynamical balance explains that the fe Method yields poorer results than Method c.

(4) Decomposing $\overline{\omega}$ into contributions from time-mean and transient eddy vorticity fluxes yields two fields that have a strong negative correlation. Therefore, using time-mean winds alone to estimate vorticity advection leads to an overestimate of $\overline{\omega}$. The effect of eddies in balancing the stretching term is important (half the mean-flow effect) and essentially of a "damping" nature (Table 4, Fig. 2).

(5) Further constraining (unnecessarily as of 1988) the vorticity flux to be a geostrophic estimate yields an $\overline{\omega}$ that is correlated to P (in a significant way) only in winter (Method g, Table 5).

(6) Combining the data for 1981–83 and 1984–86 (Method c only), geographical distributions of the correlation have been presented for 6-month long winter and summer seasons. Good correlations (< -0.6) are widespread in winter in the western one sixth of the United States and in the mid-western States.

Since we have used post-initialized data it is fair to ask what the impact of the initialization is on the results presented so far. A similar question was asked by Rosen and Salstein (1985). To their surprise, they found that for January and July 1983 Monthly Circulation Statistics based on NMC's post- and pre-initialized data are not very different (much less than the "uncertainty" expressed by the difference between ECMWF and NMC based statistics (both post initialized)). Among the more sensitive fields, $\overline{\omega}$ ranks high, and the impact of initialization in mid-latitude was reportedly of a spatial smoothing nature. We repeated the calculations underlying Tables 2–5 for several months using pre-initialized data. In Table 6, we give a detailed comparison for December 1984–86. Since only the 12 GMT data are saved for archiving in the pre-initialized shadow CDDB, we were forced to split the post-initialized data in 00 GMT and 12 GMT as well. Hence Table 6 shows results for pre-initialized 12 GMT (PR12), post-initialized 12 GMT (PO12), post-initialized 00 GMT (PO00) and the earlier results of Tables 2 to 5 (PO00 and 12 GMT). The vertical ordering is the same as in Tables 2–5. Our results are consistent with Rosen and Salstein (1985) in that the first 2 columns

Table 6. *The impact of the initialization on the correlations and interannual variabilities shown in Tables 2–5*

Previous table		PR12	PO12	PO00	PO(00 and 12 GMT)
	PC(c, P)	−46*	−40*	−61*	−61*
2	PC(c, cp)	93	87	92	90
	PC(cp, P)	−41*	−32*	−56*	−56*
3	PC(c, fe)	52	62	70	70
	PC(fe, P)	−34	−29	−55*	−53*
	PC(f, P)	−36*	−32	−48*	−43*
	PC(e, P)	19	16	−9	4
	PC(f, e)	−63	−56	−34	−64
4	RMS(f)	3.7	3.7	3.3	3.2
	RMS(e)	2.0	2.0	1.7	1.7
	RMS(fe)	2.9	3.1	3.1	2.5
	RMS(c)	2.8	1.9	2.1	1.7
	PC(a, P)	−26	−21	−43*	−35*
	PC(a, g)	76	68	78	71
5	PC(g, P)	−3	−15	−19	−18
	RMS(a)	4.3	4.3	3.5	3.5
	RMS(g)	5.7	4.8	5.0	4.6

The month is December. Shown are columns for pre-initialized fields at 12 GMT (PR12) and post-initialized fields at 12 GMT (PO12) and 00 GMT (PO00). The last column repeats results shown before in Tables 2–5 for December on 0 GMT and 12 GMT cycles. Units are % (correlation) and 10^{-2} N m^{-2} s^{-1} (RMS). The P data are identical in all correlations. The vertical ordering is the same as in Tables 2–5, see numbers on the left.

give very similar results. Hence our conclusions (1)–(6) are insensitive to the initialization. There is some indication of smoothing in that RMS (*c*) and RMS (*g*) are much less for PO12; however this "smoothing" does not improve the correlation with precipitation.

We also point out that the 00 GMT statistics (4–7 p.m. local times) give better results than the 12 GMT statistics. This could be due to the fact that the $\bar{\omega}$ data are snapshots in time while the *P* data are accumulation over time. It may be that most rain falls near 00 GMT, and/or alternatively that day-time upper air observations (used to calculate $\bar{\omega}$) are better than the 12 GMT observations (over the United States).

From Van den Dool (1987) and the update over 1984–86 (this paper) emerges the over-all conclusion that the time-mean vertical motion fields have credible patterns (at least over the United States) relying on traditional *P* data as "ground truth". This has been the case only since about 1980. Before that time the initial fields were unbalanced and the initial ω was unusable (Lau, 1979). Of course a correlation of -0.6 is not perfect but as seen in Fig. 3, the patterns in *P* and ω (Method *c*) are very similar and the correlation is "only" -0.6 because there is a lot of extra detail in the *P* field. Smoothing precipitation fields is not a trivial issue. (Calculating correlation for 48 state means does not improve the results.) Even though the initial ω is useful now we can not rule out that 6- or 12-h forecasts are still better "observations" than the initial data. Such a suggestion was made by Arpe and Klinker (1986).

Method *c* gives obviously the best results. Given all the problems with data storage, Methods *cp*, *f* etc. can only be expected to perform worse. So the reason to calculate $\bar{\omega}$ from other methods is to make a specific point, for example about geostrophic versus real wind vorticity fluxes. The most important of these points is the out of phase relationship between time-mean and transient eddy vorticity fluxes. We found this tendency both for the 3-year mean monthly flow and monthly anomalies alike. A similar relationship can be seen in model data (Mullen, 1987). The easiest interpretation (but wrong perhaps) is to see this as evidence of the damping effect that eddies have on the mean flow. In that scenario the eddies are seen to reduce the vertical motion associated with time-mean vorticity fluxes alone. However, the vorticity equation is not a maintenance equation of the type $\partial\bar{\omega}/\partial t = \text{forcing } 1 + \text{forcing } 2$ etc. Moreover we will never know what the "forcing" of $\bar{\omega}$ by the mean flow would be if the eddies had not existed. Addressing the issue of $\bar{\omega}$ forcing by eddies in a transformed system (Trenberth, 1986) would require the geostrophic assumption, which does, as we have seen, not help in terms of relating $\bar{\omega}$ to ground truth *P*. An alternative view is that a persistent vorticity anomaly is naturally advected by the mean flow and therefore everything else (including the transient eddies) has to do the opposite in order to make the vorticity tendencies zero. In fact we have found that *all* terms in the time mean vorticity equation are reducing the $\bar{u}\,\partial\bar{\zeta}/\partial x$ term (for monthly mean flow) or the $\bar{u}\,\partial\hat{\zeta}/\partial x$ term (for monthly mean anomalous flow).

No matter what the nature of the eddy-mean flow interaction exactly is, we can probably understand why monthly mean height anomaly maps are enough to infer monthly precipitation (Klein and Bloom, 1987). Given a height map, a screening procedure will select heights at a few gridpoints so as to efficiently mimic vorticity advection by the mean flow. The regression constants then take care of the damping impact of the transient eddies.

It is perhaps surprising to some readers that we never mentioned the atmospheric moisture content as a variable that ought to relate to precipitation. All attempts in Van den Dool (1987) to relate mixing ratio, moisture convergence etc. to precipitation (over 1981–83) proved futile. (This is because either the moisture analyses are useless or the availability of water vapor is not a limiting factor for precipitation in the presence of strong enough vertical motion.) Hence, we did not extend that aspect over 1984–86. We note, however, that Klein and Bloom (1987) interpret the gridpoints selected in their screening procedure in terms of moisture advection rather than vorticity advection. Nevertheless, their analysis does not explicitly use moisture data either.

It is not surprising that $\bar{\omega}$ and *P* are related, because they should, based on age-old principles of physics. But it is perhaps only since 1980 or so that we can empirically and quantitatively establish that there is such a relationship in the observations. Before 1980 large-scale data were simply not good enough to calculate divergence with enough accuracy and to link $\bar{\omega}$ successfully to quantitative precipitation measurement (still poorly known).

5. Acknowledgement

This work was supported by the Cooperative Institute for Climate Studies under NOAA Grant NA84-AA-H-00026. It is my pleasure to thank Dr. H. Savijärvi for his advice, Mr. J. Janowiak for his help in data processing and Charlene Mann for typing the manuscript. The final version benefitted from comments by Drs. M. Chelliah, W. Klein and S. Saha, as well as the anonymous reviewers.

6. Appendix

Testing significance of PC

We have applied a Monte Carlo test in order to determine the statistical significance of the pattern correlation between vertical motion (according to any of the methods) and rainfall. This is done in the following way. In eq. (1a), we correlate ω data over 1984–86 with matching P data for the same years, month and location. While leaving the ω data set as it is, we replaced the P data by 3 consecutive years (other than 84–86) from the period 1931–present over which CD data is available. By cycling through all possible choices we obtain an empirical distribution for PC with (very nearly) zero mean and standard deviation *sd*. The null hypothesis reads: ω and P are not negatively correlated. This hypothesis is rejected at the 95% level if PC (for the matching years 84–86) is less than -1.645**sd*, (one-sided t-test). All correlations involving P in Tables 2–5 were tested this way and if found significant superscripted with an asterisk. The Monte Carlo procedure is done for all months and for all estimates of $\bar{\omega}$ to be correlated with P. The empirical *sd* reflects to a large measure the spatial degrees of freedom in the ω field. Therefore, *sd* is a function of season and Method and as it so happens $\mathrm{PC}(a, P) = -0.27$ (in May Table 5) is not significant while $\mathrm{PC}(cp, P) = -0.25^*$ (in August Table 2) is.

REFERENCES

Arpe, K. and Klinker, E. 1986. Systematic errors of the ECMWF operational forecasting model in mid-latitudes. *Quart. J. R. Met. Soc. 112*, 181–202.

Eliassen, A. and Hubert, W. E. 1953. Computations of vertical motion and vorticity budget in a blocking situation. *Tellus 5*, 196–206.

Holopainen, E. O. and Oort, A. H. 1981. On the role of large-scale transient eddies in the maintenance of the vorticity and enstrophy of the time-mean atmospheric flow. *J. Atmos. Sci. 38*, 270–280.

Holton, J. R. 1979. *An introduction to dynamical meteorology*. New York: Academic Press, 391 pp.

Hoskins, B. J. and Sardeshmukh, P.D. 1987. Transient eddies and the seasonal mean rotational flow. *J. Atmos. Sci. 44*, 328–338.

Hoskins, B. J., Draghici, I. and Davies, H. C. 1978. A new look at the ω-equation. *Quart. Meteor. Soc. 104*, 31–38.

Janowiak, J. E., Ropelewski, C. F. and Halpert, M. S. 1986. The precipitation anomaly classification: A method for monitoring regional precipitation deficiency and excess on a global scale. *J. Climate Appl. Meteor. 25*, 565–574.

Klein, W. H. and Bloom, H. J. 1987. Specification of monthly precipitation over the United States from the surrounding 700 mb height field in winter. *Mon. Wea. Rev. 115*, 2118–2132.

Lau, N.-C. 1979. The structure and energetics of transient disturbances in the Northern Hemisphere wintertime circulation. *J. Atmos. Sci. 36*, 982–995.

Mullen, S. L. 1986. The local balances of vorticity and heat for blocking anticyclones in a spectral general circulation model. *J. Atmos. Sci. 43*, 1406–1441.

Mullen, S. L. 1987. Transient eddy forcing of blocking flows. *J. Atmos. Sci. 44*, 3–22.

Opsteegh, J. D. and Van den Dool, H. M. 1979. A diagnostic study of the time mean atmosphere over Northwestern Europe during winter. *J. Atmos. Sci. 36*, 1862–1879.

Palmén, E. and Newton, C. W. 1969. Atmospheric Circulation Statistics. International Geophysical Series, vol. 13. New York: Academic Press, 603 pp.

Rosen, D. R. and Salstein, D. A. 1985. Effect of initialization on diagnoses of NMC large-scale circulation statistics. *Mon. Wea. Rev. 113*, 1321–1337.

Sardeshmukh, P. D. and Hoskins, B. J. 1987. On the derivation of the divergent flow from the rotational flow: the χ problem. *Q. J. R. Meteorol. Soc. 113*, 339–360.

Savijärvi, H. 1977. The interaction of the monthly mean flow and large-scale transient eddies in two different circulation types. Part 2: Vorticity and temperature balance. *Geophysika 15*, 207–230.

Trenberth, K. E. 1986. An assessment of the impact of transient eddies on the zonal flow during a blocking episode using localized Eliassen-Palm diagnostics. *J. Atmos. Sci. 43*, 2070–2087.

Van den Dool, H. M. 1987. An empirical study on the parameterization of precipitation in a model of the time mean atmosphere. *J. Atmos. Sci. 44*, 224–235.

White, G. H. 1983. Estimates of the seasonal mean vertical velocity fields of the extratropical Northern Hemisphere. *Mon. Wea. Rev. 111*, 1418–1433.

Zamora, R. J., Shapiro, M. A. and Doswell, C. A. 1987. The diagnostis of upper tropospheric divergence and ageostrophic wind using profiler wind observations. *Mon. Wea. Rev. 115*, 871–884.

Zwack, P. and Okossi, B. 1986. A new method for solving the quasi-geostrophic omega equation by incorporating surface pressure tendency data. *Mon. Wea. Rev. 114*, 655–666.